Proceedings of International Structural Engineering and Construction, 8(1), 2021
Interdisciplinary Civil and Construction Engineering Projects
Edited by El Baradei, S., Abodonya, A., Singh, A., and Yazdani, S.

ISSN: 2644-108X
www.doi.org/10.14455/ISEC.2021.8(1).GFE-01

ON THE SHEAR STIFFNESS DECREASE OF SANDY SOILS DUE TO PARTICLE CRUSHING PROGRESS

HARUYUKI YAMAMOTO

Division of Development Science, Hiroshima University/IDEC, Higashi-Hiroshima, Japan

Many previous studies have focused on theoretical and experimental evaluations of the crushing of sandy soil particles under high pressure conditions. From the perspective of practical scenarios, the decreased bearing capacity caused by volume shrinkage and the reduced shear strength and stiffness caused by the crushing of sandy soil particles are important aspects. Therefore, this study aims to confirm the decrease in the shear stiffness of sandy soils subjected to various stress levels combined with high principal stresses. Author conducted crushing tests using the high-pressure true tri-axial compression apparatus under the planned stress paths. Tests on isotropic compression without deviatoric stress q and those involving combinations of the mean stress p and deviatoric stress q up to the shear failure line (SFL) on the p - q plane are employed to characterize the particle crushing of sandy soils. The results indicate that the shear stiffness of sandy soils starts to decrease due to particle crushing under a combination of low mean stress p and high deviatoric stress q. Furthermore, experimental formulas regarding the decrease in shear stiffness due to particle crushing were estimated based on the relationships among the mean stress p, deviatoric stress q and deviatoric strain ε_d.

Keywords: Tri-axial compression, High pressure, Stress path, Mean stress, Deviatoric stress, Deviatoric strain, Experimental formula.

1 INTRODUCTION

Over the years, quite a number of experimental and analytical studies have been conducted on the compressibility of sandy soils and the bearing capacity of piles. However, most of these studies have been conducted with relatively solid grounds of hard soil particles in mind, and there seems to be a paucity of studies on the bearing capacity of the piles for the ground consisting of soil particles that are highly crushable and become compressible rapidly due to crushing (Yasufuku *et al*. 1994). Therefore, it is of great significance from an engineering point of view to clarify the strength–deformation properties of soil with such compressibility or crushability in order to establish a rational design method for deep foundations.

On the other hand, triaxial and one-dimensional compression tests have been used by a number of researchers to study the mechanical behavior and crushing properties of granular materials (Miura and Yamanouchi 1977, Yasufuku *et al*. 1994, Yamamuro *et al*. 1996, Vilhar *et al*. 2013). In the one-dimensional compression test, specimens are treated as the K_0 state because the loading test is performed with the lateral deformation of the specimens fully constrained. This test is intended for the area in the ground immediately below the center of the pile tip where no shear failure occurs and does not consider particle crushing induced by shear failure at the periphery of the pile tip. The particle crushing phenomenon is more prominent directly below the corner edge of the pile tip where shear failure occurs than immediately below the center of the

pile tip; therefore, it is desirable to accumulate more study results on the crushing phenomenon under the combined stresses of mean stress p and deviatoric stress q.

Therefore, this study considers the effect of particle crushing on the shear stiffness of granular materials by performing crushing tests using a rigid plate loading high-pressure compression apparatus capable of independently controlling the mean stress p and deviatoric stress q.

2 EXPERIMENTAL OVERVIEW

In this study, author have developed and fabricated a high-pressure compression apparatus capable of performing true triaxial stress control using rigid plates to achieve particle crushing that occurs under high-pressure conditions (Yokura *et al*. 2015). As shown in Figure 1, a cubic-shaped test specimen measuring 50 × 50 × 50 mm with flattened corners was installed at the center of the apparatus. The test specimen was loaded by a hydraulic jack capable of pressurizing up to 200 MPa through the loading rod. The movable parts of the loading apparatus were all supported by ball bushings and moved freely without frictional resistance. Since one of the two loading rods facing each other was loaded using the reaction force of the other loading rod, equal pressure could be applied to both rods at the same time; the displacement is approximately equal between the two rods unless there is friction at the ball bushing. In the vertical direction, the weight of the loading apparatus and the loading rods was supported by the weight through a pulley, such that the loads from the two opposing loading rods were equal, as in the case with two horizontal directions. In addition, ultra-thin Teflon sheets were attached using silicone grease to the end faces of the loading rods to reduce the frictional resistance between test specimens.

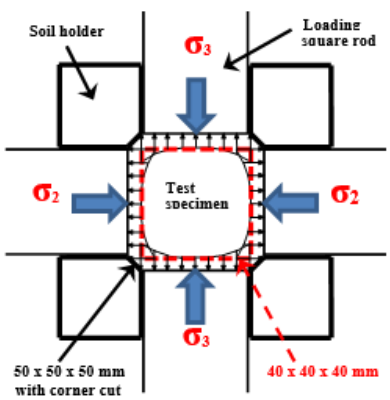

Figure 1. Plan view of test specimen.

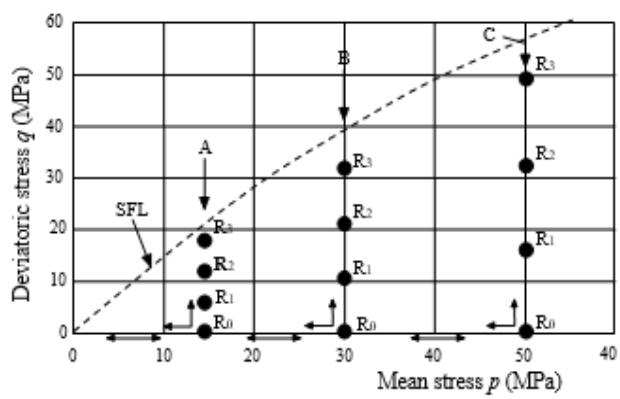

Figure 2. Stress-path patterns on the p-q plane.

Toyoura silica sand, which is commonly used in various soil tests, was used in this study. Toyoura silica sand consists of round particles of almost uniform size, and most of its composition is silica (SiO_2). A grain size test of Toyoura sand by a general method showed that the weight ratio of the particles in the 125–297 μm rang was large and that almost no particles smaller than 74 μm in diameter were found. A special container designed to prevent sand particles from spilling out was installed at the center of the apparatus. Then, sand was placed in the container to make test specimens. The test specimens were divided into approximately 10 layers, and each layer was tamped down and compacted to achieve a relative density of 90% or more.

It is desirable to use parameters that can express the mean stress, representing the confining pressure component, and the deviation stress, representing the shear stress component, to indicate the stress paths for tracing the mechanical behavior of a frictional material such as sand. Therefore, in this study, stress paths were represented with the *p*-*q* plane using the mean stress *p* and deviatoric stress *q*. The definitions of the mean stress *p* and deviatoric stress *q* are shown in Eqs. (1) and (2), respectively:

$$p = \frac{1}{3}\left(\sigma_1 + \sigma_2 + \sigma_3\right) \tag{1}$$

$$q = \frac{1}{\sqrt{2}}\sqrt{\left(\sigma_1 - \sigma_2\right)^2 + \left(\sigma_2 - \sigma_3\right)^2 + \left(\sigma_3 - \sigma_1\right)^2} \tag{2}$$

The results of preliminary experiments showed that the intermediate principal stress σ_2 had little effect on the crushing of Toyoura silica sand (Fukuda and Yamamoto 2018), so the crushing tests were conducted under the condition of $\sigma_2 = \sigma_3$ (triaxial compression condition). Under triaxial compression conditions, using the mean stress *p* and deviatoric stress *q* as well as the shear resistance angle (internal friction angle) φ, the Mohr–Coulomb's shear failure criterion is expressed as Eq. (3).

$$q = \frac{6sin(\ )}{3\text{-}sin(\ )}\ p \tag{3}$$

The equation represents the SFL in the *p* - *q* plane, which is actually an upper convex curve as shown in Figure 2, showing that the internal friction angle gradually decreases with an increase in the mean stress *p* and deviatoric stress *q*. The SFL is defined as a series of values of deviatoric stress *q* at the point where the displacement in the maximum principal stress σ_1 direction starts to increase sharply and σ_1 almost stops increasing. Figure 2 also shows the stress paths established in this test. First, three cases of isotropic compression tests (A, B, C–R_0) were carried out. Then nine cases of shear crushing tests (A, B, C–$R_{1,\ 2,\ 3}$) were performed, in which deviatoric stress was applied with the mean stress *p* kept constant after the sand was isotropically compressed. The positions of the black dots in the figure 2 represent the action levels of the maximum mean stresses (A, B, and C) and the maximum deviatoric stresses ($R_{0,\ 1,\ 2,\ 3}$) in each test. After applying the load to the specimens up to these levels, the load was removed following the same stress path in each test. The action level of mean stress was within the expected range in the ground near the tip of the bearing pile, and the action levels of deviatoric stress were R_1 and R_2, which were almost equally divided between R_3 and isotropic compression R_0 .

3 EXPERIMENTAL RESULTS AND DISCUSSIONS

Figure 3 shows a comparison of the grain-size accumulation curves before and after the crushing test. Since only the sieve analysis test was performed for particle size analysis and no sedimentation analysis was performed for fine particles, components smaller than 0.074 mm are not shown. These figures clearly show that the particle crushing progresses more significantly and the fine fraction increases with an increase in the mean stress *p* and the deviatoric stress *q*.

Figure 4 shows an example of the relationship between the deviatoric stress *q* and deviatoric strain ε_d when the deviatoric stress *q* is increased and decreased after the mean stress *p* is kept constant. The deviation strain ε_d is expressed in Eq. (4), where ε_1, ε_2 and ε_3 represent the principal strain components in the three-dimensional strain space. The ε_d^p and ε_d^e in Figure 4 are the non-

recovering (plastic) and recovering (elastic) components, respectively. The plastic and elastic components are evaluated separately because the relationship between the deviatoric stress q and the deviatoric strain ε_d, when the deviatoric stress q increases, has a nonlinearity from the beginning and it is difficult to identify its gradient directly. The relationship between the normal shear stiffness G and the shear stiffness G' with respect to the relationship between the deviatoric stress q and deviatoric strain ε_d is shown in Eq. (5).

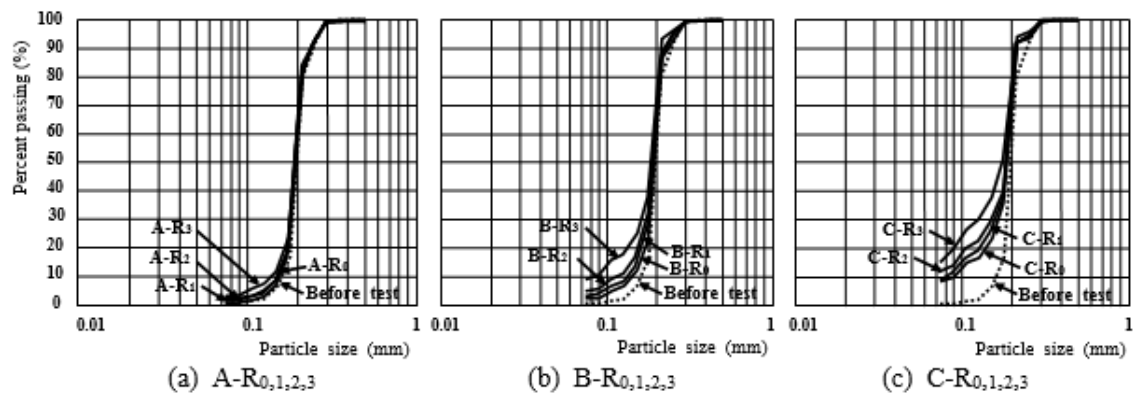

Figure 3. Grain-size accumulation curves before and after crushing test.

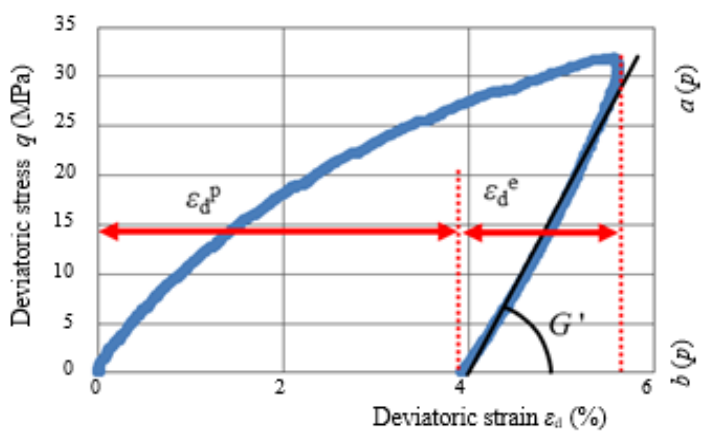

Figure 4. Example (B-R_3) of relationship between deviatoric stress q and deviatoric strain ε_d.

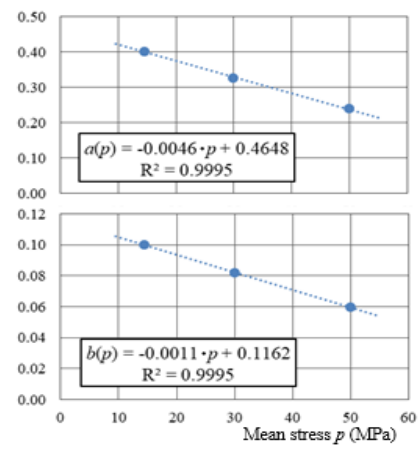

Figure 5. Relationship between $a(p)$, $b(p)$ and mean stress p.

$$\frac{q}{\varepsilon_d} = 3G = G' \tag{4}$$

$$\varepsilon_d = \frac{\sqrt{2}}{3} \cdot \sqrt{(\varepsilon_1 - \varepsilon_2)^2 + (\varepsilon_2 - \varepsilon_3)^2 + (\varepsilon_3 - \varepsilon_1)^2} \tag{5}$$

The necessary conditions for the estimation of deviatoric plastic strain ε_d^p are that the strain does not occur unless acted upon by deviatoric stress ($\varepsilon_d^p = 0$ when $q = 0$) and that the deviatoric plastic strain gradually increases as the deviatoric stress increases. Based on these conditions, the possible experimental estimation equations are formulated as Eqs. (6), (7) and (8). Eqs. (7) and (8) are set up as linear functions of p because the difference in the confining pressure may affect

$a(p)$ and $b(p)$ in Eq. (6). Therefore, the unknown coefficients of the equations $a(p)$ and $b(p)$ (A_1, A_2, B_1 and B_2) are determined by the least squares method and are shown in Figures 5. Figure 6 compares the values obtained from these experimental estimation equations (solid lines) with the values obtained in this experiment (dots). Although some amount of scatter is seen in the experimental values, it is well approximated that the plastic deviatoric strain ε_d^p rapidly increases with an increase in the deviatoric stress q. These results also show that the deviatoric plastic strain ε_d^p tends to decrease with an increase in the mean stress p.

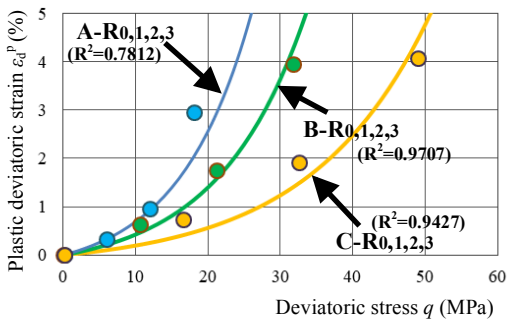

Figure 6. Relationship between plastic deviatoric strain ε_d^p and deviatoric stress q.

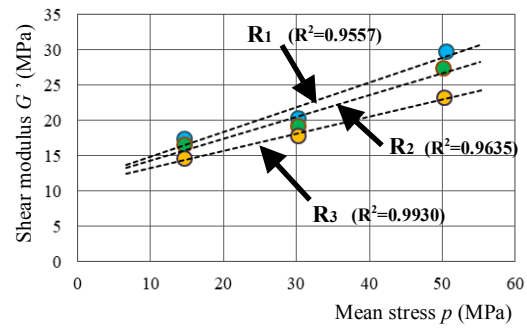

Figure 7. Relationship between shear modulus G' and mean stress p.

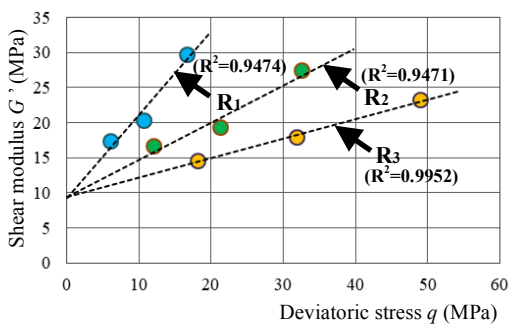

Figure 8. Relationship between shear modulus G' and deviatoric stress q.

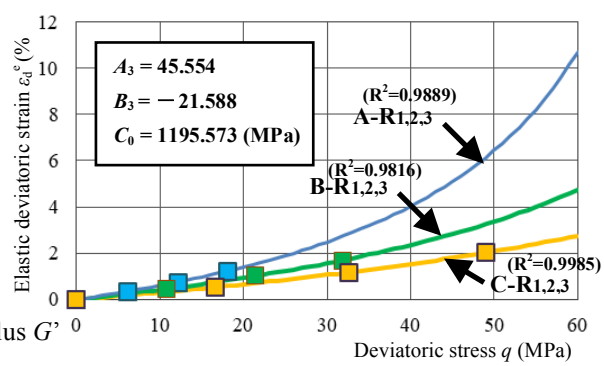

Figure 9. Relationship between elastic deviatoric strain ε_d^e and deviatoric stress q.

$$\varepsilon_d^p = a(p) \cdot \left(e^{b(p) \cdot q} - 1\right) \tag{6}$$

$$a(p) = A_1 \cdot p + A_2 \tag{7}$$

$$b(p) = B_1 \cdot p + B_2 \tag{8}$$

The elastic deviatoric strain ε_d^e is defined as the elastic component of the deviatoric strain, which disappears as the load is removed, and can be rewritten from Eq. (5) to as Eq. (9). Figures 7 and 8 show the relationship between the shear modulus G' and the mean stress p and the deviatoric stress q, respectively. These figures show that there is a linear relationship in both cases; therefore, the experimental estimation equation for G' is assumed as Eq. (10) and the unknown coefficients (A_3, B_3, and C_0) are determined by the least squares method.

$$\varepsilon_d^e = \frac{1}{G'} \cdot q \tag{9}$$

$$G' = A_3 \cdot p + B_3 \cdot q + C_0 \tag{10}$$

Figure 9 shows a comparison between the values obtained from this experimental estimation equation (solid lines) and the values obtained from the actual experiment (dots). The figure shows that the experimental values are very accurate approximations. However, additional experimental data pertaining to particle crushing are required to formulate highly accurate estimation equations, because a certain amount of inevitable scatter exists in the experimental data.

By adding Eqs. (6) and (9), the deviatoric strain ε_d is obtained; as shown in Figures 6 and 9, the increasing deviatoric strain (decreasing shear stiffness) with the progression of particle crushing can be evaluated as a function of the mean stress p and the deviatoric stress q.

4 CONCLUSIONS

In this study, crushing tests of Toyoura silica sand were conducted using a rigid plate-type high-pressure compression apparatus capable of independently controlling true triaxial stresses and the shear stiffness of the sand with the development of crushing was discussed. Deviatoric strains obtained from crushing experiments were separated into plastic and elastic components and approximate function expressions consisting of mean stress p and deviatoric stress q were established for each component. The deviatoric strains estimated from these approximate functions are consistent with experimental values; the changes in shear stiffness, which decrease with the progress of particle crushing, could be estimated from the mean stress p and the deviatoric stress q. However, these results were derived from the crushing test results when the mean stress p was kept constant and only the deviatoric stress q was increased or decreased. It is necessary to study the applicability of the results to the stress paths, where the mean stress p and the deviatoric stress q vary at the same time, and to other granular materials.

Acknowledgments

This study was supported by JSPS KAKENHI Grant Number JP19K04690.

References

Fukuda, K., and Yamamoto, H., *Crushing characteristics of soil particle on the effect of stress path*, Proceedings of International Structural Engineering and Construction (ASEA-SEC-4), 5(2), GFE-02, 1-6, December, 2018.

Miura, N., and Yamanouchi, T., *Effect of particle-crushing on the shear characteristics of a sand*, Proc. JSCE, 260,109-118, April, 1977 (in Japanese).

Vilhar, G., Jovicic, V. and Coop, M. R., *The role of particle breakage in the mechanics of a non-plastic silty sand*, Soils and Foundations, 53(1), 91-104, 2013.

Yamamuro, J. A., Bopp, P. A. and Lade, P. V., *One-Dimensional Compression of Sands at High Pressures*, Journal of Geotechnical Engineering, 122(2), 147-154, 1996.

Yasufuku, N., Tanaka, K., Murata, H. and Hyodo, M., *End bearing capacity of pile in highly compressible sands and its evaluation*, Doboku Gakkai Ronbunshu, JSCE, 505(III-29), 191-200, December, 1994 (in Japanese).

Yokura, K., Yamamoto, H., and Wu, Y., *Crushing tests of soil particles by high pressure true tri-axial compression apparatus*, The 6th Japan-China Geotechnical Symposium, Sapporo, Japan, 51-56, 2015.